Empirical Time-Dimension Model of Spectrum Use Based on a Discrete-Time Markov Chain With Deterministic and Stochastic Duty Cycle Models

Miguel López-Benítez, *Student Member, IEEE*, and Fernando Casadevall, *Member, IEEE*

Abstract—The spectrum occupancy models widely used to date in dynamic spectrum access/cognitive radio (DSA/CR) research frequently rely on assumptions and oversimplifications that have not been validated with empirical measurement data. In this context, this paper presents an empirical time-dimension model of spectrum use that is appropriate for DSA/CR studies. Concretely, a two-state discrete-time Markov chain with novel deterministic and stochastic duty cycle models is proposed as an adequate mean to accurately describe spectrum occupancy in the time domain. The validity and accuracy of the proposed modeling approach is evaluated and corroborated with extensive empirical data from a multiband spectrum measurement campaign. The obtained results demonstrate that the proposed approach is able to accurately capture and reproduce the relevant statistical properties of spectrum use observed in real-world channels of various radio technologies. The importance of accurately modeling spectrum use in the design and evaluation of novel DSA/CR techniques is highlighted with a practical case study.

Index Terms—Cognitive radio (CR), dynamic spectrum access (DSA), spectrum usage models, time dimension.

I. INTRODUCTION

THE OWNED spectrum allocation policy, which has been in use since the early days of modern radio communications, assigns fixed spectrum bands to particular wireless standards. Such bands are further divided into subbands that are allocated under static licenses and solely remain for the exclusive use of the licensee. This allocation policy has been proven to effectively control interference among radio communication systems and simplify the design of hardware for use at a known and fixed range of frequencies. However, the overwhelming proliferation of new operators, innovative services, and wireless technologies during the last years has resulted, under this static regulatory regime, in the depletion of all spectrum bands with commercially attractive radio propagation characteristics. The vast majority of spectrum bands regarded as usable have been already allocated, thus hindering the commercial rollout of new emerging services.

An important number of spectrum measurement campaigns covering wide frequency ranges [1]–[13], as well as some specific licensed bands [14]–[20], have been carried out all over the world to determine the degree to which allocated spectrum bands are used in real wireless communication systems. Empirical measurements have demonstrated that the spectrum is mostly underutilized, thus indicating that the virtual spectrum scarcity problem actually results from static and inflexible spectrum management policies rather than the physical scarcity of usable radio frequencies. The owned spectrum allocation policy was once appropriate, but nowadays, it has become obsolete, and new spectrum management paradigms are therefore required to efficiently exploit the precious radio resources. This situation has motivated the emergence of more flexible spectrum access policies [21]–[23]. In this context, the dynamic spectrum access (DSA) principle [24], which is based on the cognitive radio (CR) paradigm [25], [26], has gained popularity as a promising solution to conciliate the existing conflicts between the ever-increasing spectrum demand growth and the currently inefficient spectrum utilization.

The basic underlying idea of DSA/CR is to allow unlicensed (secondary) users to access in an opportunistic and noninterfering manner some licensed bands temporarily unoccupied by licensed (primary) users. Unlicensed secondary terminals monitor the spectrum to identify time gaps left unused by primary users, which are usually referred to as *white spaces* or *spectrum holes* [27], place secondary transmissions within such spaces, and vacate the channel as soon as primary users return. Secondary unlicensed transmissions are allowed to follow this operating principle as long as they do not result in harmful interference to primary radios.

Due to the opportunistic nature of the DSA/CR principle, the behavior and performance of a secondary network depends on the spectrum occupancy patterns of the primary system. Realistic and accurate modeling of such patterns therefore becomes essential and extremely useful in the domain of DSA/CR research. The potential applicability of spectrum use models ranges from analytical studies to the design and dimensioning of secondary networks, as well as the development of innovative simulation tools and more efficient DSA techniques for wireless communication systems where the DSA/CR technology can be applied, including heterogeneous wireless access

The authors are with the Department of Signal Theory and Communications, Universitat Politècnica de Catalunya, 08034 Barcelona, Spain (e-mail: miguel.lopez@tsc.upc.edu; ferranc@tsc.upc.edu).

systems [28] and vehicular networks [29]–[31]. Nevertheless, the utility of such models depends on their realism and accuracy. Unfortunately, the models for spectrum use commonly used to date in DSA/CR research are limited in scope and based on oversimplifications or assumptions that have not been validated with empirical measurement data. Spectrum occupancy modeling in the context of DSA/CR constitutes a rather unexplored research area that still requires more effort.

The problem of modeling spectrum occupancy in the spatial dimension was addressed in [32] and [33]. This paper focuses on the time domain of spectrum usage and extends previous work [34]. In particular, a two-state discrete-time Markov chain (DTMC) with deterministic and stochastic duty cycle (DC) models is proposed as an adequate mean to accurately describe spectrum occupancy in the time domain. The validity and correctness of the model developed in this paper is evaluated and corroborated with extensive empirical measurement results for various frequency bands and radio technologies. The obtained results demonstrate that the proposed approach is able to capture and reproduce with significant accuracy the statistical properties of spectrum use observed in real-world channels.

The remainder of this paper is organized as follows: First, Section II reviews the existing related work on time-dimension models of spectrum use, identifying the existing deficiencies that motivate this paper. Section III describes the measurement setup and methodology employed to capture the empirical data used in the validation of the proposed model. Section IV presents the traditional Markov chain model commonly used in previous literature. Since such Markov model is not able to accurately capture and reproduce all the relevant statistical properties of spectrum use in the time domain, it is extended with adequate deterministic and stochastic DC models, which are presented in Sections V and VI, respectively. The validity and accuracy of the developed model is assessed and verified in Section VII. The importance of disposing of accurate models of spectrum use, such as that presented in this paper, for the design and evaluation of novel DSA/CR techniques is highlighted with a practical case study in Section VIII. Finally, Section IX summarizes the research carried out in this paper.

II. RELATED WORK AND MOTIVATION

A. Previous Work Based on CTMCs

From the point of view of a DSA/CR network, spectrum use can adequately be modeled by means of a Markov chain with two states: one indicating that the channel is busy (i.e., used by a primary user and therefore not available for opportunistic access) and the other one indicating that it is idle (i.e., available for secondary use). A popular channel model in DSA/CR research is the well-known two-state continuous-time Markov chain (CTMC) model, where the channel remains in one state for a random time period before switching to the other state. The *state holding time* or *sojourn time* is modeled as an exponentially distributed random variable.

The CTMC model has widely been employed in the study of various aspects of DSA/CR networks such as medium-access control (MAC) protocols for spectrum sharing [35], [36], MAC-

layer sensing schemes [37]–[39], adaptive spectrum-sensing solutions [40], the sensing–throughput tradeoff [41], [42], and the performance of DSA/CR sensor networks [43].

Although the CTMC model has been widely used in the literature, some studies based on empirical measurements [44]–[48] have demonstrated that state holding times are not exponentially distributed in practice. In particular, it was found that state holding times are more adequately described by means of generalized Pareto [44], a mixture of uniform and generalized Pareto [45], [46], hyper-Erlang [45], [46], generalized Pareto and hyperexponential [47], as well as geometric and lognormal [48] distributions. Based on the conclusions from previous modeling studies, a more appropriate model is therefore the continuous-time semi-Markov chain (CTSMC) model, where the state holding times can follow any arbitrary distribution. As a result, some studies have considered CTSMC models. This is the case, for instance, of [49] and [50], which consider a CTSMC model where the busy/idle periods are exponentially/Erlang distributed, respectively.

B. Previous Work Based on DTMCs

In the two-state DTMC model, the time index set is discrete. According to this model, the channel remains in a certain state at each step, with the state randomly changing between steps. The behavior of the channel is described by means of a set of transition probabilities between states.

The DTMC model has been widely used in the DSA/CR literature as well. For instance, it has been used to analyze the performance of MAC [51] and joint MAC/sensing [52] frameworks for opportunistic spectrum access, dynamic channel selection strategies [53], opportunistic scheduling policies [54], channel selection schemes [55] based on the interference temperature model [56], and the voice-service capacity of DSA/CR systems under both ideal [57] and imperfect [58] spectrum-sensing conditions, as well as under quality-of-service restrictions [59].

As opposed to the continuous-time case, and to the best of the authors' knowledge, the suitability of the DTMC channel model in describing the statistical properties of spectrum occupancy patterns in real systems has not been evaluated and assessed in the literature before.[1] This means that an important volume of research in DSA/CR has been based on assumptions or oversimplifications that have not been validated with empirical measurement data and, more importantly, that future research studies based on the DTMC channel model will also suffer from the same drawback due to the nonexistence of appropriate DTMC modeling approaches capable of capturing the relevant statistical properties of spectrum occupancy in the time domain. In this context, this paper covers such deficiencies and fills the existing gaps by evaluating the ability of the DTMC model to reproduce the statistical properties of spectrum use in real radio communication systems and extending the conventional

---

[1]A DTMC model could be characterized by discrete-time distributions for state holding times instead of a set of transition probabilities between states. Whereas the former approach has received some attention [48], the latter, which has been widely employed in the literature, remains unexplored and is studied in this paper.
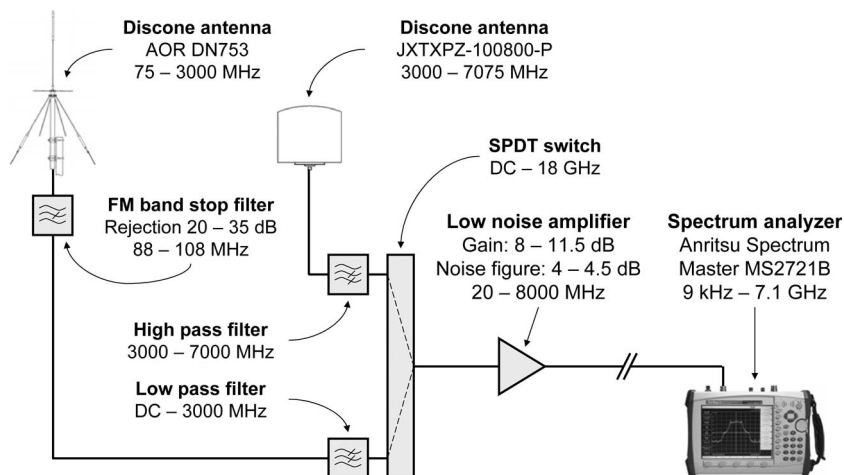
Fig. 1. Measurement setup employed in this paper.

DTMC model with appropriate deterministic and stochastic DC models.

III. MEASUREMENT SETUP AND METHODOLOGY

The employed measurement configuration (see Fig. 1) relies on a spectrum analyzer setup where different external devices have been added to improve the detection capabilities and, hence, the accuracy and reliability of measurements. The design is composed of two broadband discone-type antennas covering the frequency range from 75 to 7075 MHz; a single-pole double-throw switch to select the desired antenna; several filters to remove undesired overloading (FM) and out-of-band signals; a low-noise preamplifier to enhance the overall sensitivity and, thus, the ability to detect weak signals; and a high-performance spectrum analyzer to record the spectral activity. The spectrum analyzer is connected to a laptop via Ethernet and controlled using the MATLAB's Instrument Control Toolbox. Tailor-made software controls all the measurement process by means of commands in Standard Commands for Programmable Instruments format using the Virtual Instrument Standard Architecture standard and Transmission Control Protocol/Internet Protocol interface.

Various spectrum bands (see Table I) were measured from our department's building at the Universitat Politècnica de Catalunya, Campus Nord, in a urban environment in Barcelona, Spain (latitude $41°23'20''$N, longitude $2°6'43''$E, and altitude 175 m). Most of the measured bands were analyzed in the selected building's rooftop, which represents a strategic location with direct line-of-sight to several transmitting stations located a few tens or hundreds of meters away from the antenna and without buildings blocking the radio propagation. The measurement equipment was placed inside the building, however, for the Digital Enhanced Cordless Telecommunication (DECT) and Industrial, Scientific, and Medical (ISM) bands since they are used by short-range radio technologies more commonly deployed in indoor environments. These measurement locations were carefully selected to maximize the receiving signal-to-noise ratio and, hence, ensure a reliable and accurate estimation of the true busy/idle states for the channels of the measured

TABLE I
SPECTRUM BANDS MEASURED IN THIS PAPER

Measured band	Frequency (MHz)	No. of channels	No. of samples	Avg. sweep time (secs)
TETRA UL	410–420	399	199013	3.04
TETRA DL	420–430	399	195956	3.08
E-GSM 900 UL	880–915	174	156460	3.86
E-GSM 900 DL	925–960	174	158147	3.82
DCS 1800 UL	1710–1785	374	125986	4.80
DCS 1800 DL	1805–1880	374	128615	4.70
DECT	1880–1900	10	178388	3.39
ISM	2400–2500	13	105940	5.70

bands. Although this paper does not present results for all the spectrum bands shown in Table I, the proposed model was developed and validated based on channels from all the measured bands and radio technologies.

Each band was measured across a time span of 7 days, from Monday midnight to Sunday midnight. This measurement period enabled us not only to capture a high number of signal samples (see Table I) but to appreciate any potential pattern on spectrum use as well (e.g., channel usage variations between weekdays and weekends, as well as variations at different times along days/nights). Measurements were performed using average detection and with a resolution bandwidth of 10 kHz, which allows resolving signals in frequency, even for narrow-band technologies such as Terrestrial Trunked Radio (TETRA) and Global System for Mobile Communications (GSM)/Digital Cellular System (DCS). The external amplifier shown in Fig. 1, along with the spectrum analyzer's internal amplifier ($\approx$25-dB gain), results in an overall sensitivity value around -130 dBm/10 kHz, which guarantees a reliable estimation of the true spectrum occupancy.

Before validating the proposed model with the captured empirical data, it was first necessary to extract the binary channel occupancy pattern by determining which power samples measured by the spectrum analyzer correspond to busy channels and which others to idle channels. To detect whether a channel is used by a licensed user, a number of different signal detection methods, which are referred to as *spectrum-sensing* algorithms in the context of DSA/CR, have been proposed in the literature [60]–[62]. The existing solutions provide different tradeoffs

among required sensing time, complexity, and detection capabilities. Their practical applicability, however, depends on how much information is available about the primary user signal. In the most generic case, no prior information is available. If only low time-resolution power measurements of the spectrum utilization are available, the application of advanced techniques such as feature detection methods results infeasible, and the energy detection method is the only possibility left [63], which is able to work irrespective of the signal to be detected. Due to its simplicity and relevance to the processing of power measurements, energy detection has been a preferred approach for many past spectrum studies and constitutes the spectrum-sensing method considered in this paper. Energy detection compares the received signal energy in a certain channel to a properly set decision threshold.[2] If the signal lies above the threshold, the channel is declared to be busy (i.e., occupied by the licensed system). Otherwise, the channel is supposed to be idle (i.e., available for secondary usage). Following this principle, the power samples measured for each channel were mapped to binary busy/idle states. Based on the resulting binary sequences, the lengths of busy and idle periods were extracted, and the proposed DTMC channel model was validated with empirical data.

It is worth noting that the average sweep times shown in Table I indicate that the resulting sampling rates of swept spectrum analyzers are not comparable with those of the measurement equipment employed in other modeling studies [44]–[47], which may result in undersampling of the measured signals and, thus, the misdetection of channel state changes between consecutive channel observations. The binary occupancy pattern observed in such a case, although inaccurate, is still interesting and useful due to two main reasons. The first reason is that such binary pattern can be thought of as the occupancy perception of a DSA/CR user that periodically senses the channel and observes its state at discrete-time instants. Therefore, spectrum analyzer measurements are useful to model spectrum occupancy from the point of view of the DSA/CR user perception. Since the overall behavior of a DSA/CR network is driven by the primary occupancy pattern as perceived by the sensing nodes, analytical studies and simulations of DSA/CR systems should rely on spectrum use models that are able to accurately capture and reproduce the channel occupancy pattern in real channels, as observed by DSA/CR terminals. On the other hand, short idle periods resulting from bursty data transmissions are difficult to exploit for secondary usage in practice,[3] which, from a practical point of view, is equivalent to a busy channel state. Exploitable idle periods normally arise when there is no primary user making use of the channel, which can be reliably
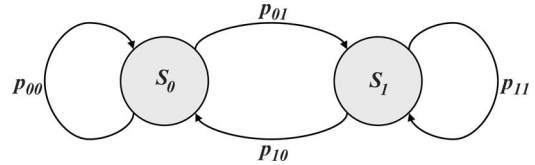

Fig. 2.   DTMC model.

detected with a spectrum analyzer within reasonable accuracy limits in spite of its limited time resolution. Moreover, it is worth noting that spectrum analyzers have been successfully applied in previous modeling studies [48] and have the advantage of enabling high dynamic ranges, high sensitivity levels, and wideband measurements. The empirical data captured for various radio technologies enabled an adequate validation of the model developed in this paper.

A more detailed and in-depth description of the employed measurement setup and its configuration, as well as the considered methodological procedures, can be found in [64] and [65].

IV. DICRETE-TIME MARKOV CHAIN

At a given time instant, a primary radio channel may be either busy or idle, meaning that the temporal spectrum occupancy pattern of a primary radio channel can be adequately modeled by means of a two-state Markov chain. Let us denote, by $\mathbb{S} = \{s_0, s_1\}$, the space state for a primary radio channel, where the s_0 state indicates that the channel is idle, and the s_1 state indicates that the channel is busy. Channel state $S(t)$ at time t can be either $S(t) = s_0$ or $S(t) = s_1$. As discussed in Section II, this paper focuses on the particular case of DTMCs, where the time index set is discrete, i.e., $t = t_k = kT_s$, where k is a nonnegative integer representing the step number and T_s is the time period between consecutive transitions or state changes.[4] The behavior of a DTMC can be described by means of a set of transition probabilities between states (see Fig. 2), which can be expressed in matrix form as

$$\mathbf{P} = \begin{bmatrix} p_{00} & p_{01} \\ p_{10} & p_{11} \end{bmatrix} \tag{1}$$

where p_{ij} represents the probability that the system transitions from state s_i to state s_j. Note that the channel model commonly used in previous work assumes a stationary (time-homogeneous) DTMC, where transition matrix $\mathbf{P}$ is constant and independent of time instant t.

The DC of a channel, henceforth denoted by Ψ, is a very straightforward metric, and an accurate reproduction is a minimum requirement for any time-dimension model of spectrum use. The DC can be defined from both probabilistic and empirical perspectives. Whereas the former results are more appropriate for theoretical analyses, the latter results are more convenient for validation with empirical data. From an empirical viewpoint, the DC can be estimated as the fraction of time that the channel is declared to be busy based on the procedure described in Section III. From a probabilistic viewpoint, the DC can be defined as the probability that the channel is busy. The

---

[2]To determine the decision threshold, the antenna in Fig. 1 was replaced with a matched load to measure the system noise. For each measured channel, the threshold was then set as the maximum noise power measured plus a 3-dB margin to avoid false alarms. On the other hand, the high signal-to-noise ratio conditions under which most of the measured signals were received guarantee that the probability of misdetection is minimized, thus resulting in a nearly ideal detection performance under such conditions.

[3]For instance, the time-slot duration is 14.167 ms in TETRA, 577 μs in GSM/DCS, and 417 μs in DECT. The IEEE 802.11 protocol, which is used by wireless local area networks operating in the ISM band, defines interframe spaces on the order of 50 μs or less.

[4]T_s can be associated to the average sweep times shown in Table I.

probabilities that the model in Fig. 2 is in each of its states in the long term are given by [66]

$$P(S = s_0) = \frac{p_{10}}{p_{01} + p_{10}} = 1 - \Psi \qquad (2)$$

$$P(S = s_1) = \frac{p_{01}}{p_{01} + p_{10}} = \Psi. \qquad (3)$$

Thus, the DTMC model can be configured to reproduce any arbitrary DC Ψ by selecting the transition probabilities as $p_{01} = p_{11} = \Psi$ and $p_{10} = p_{00} = 1 - \Psi$, which yields

$$\mathbf{P} = \begin{bmatrix} 1 - \Psi & \Psi \\ 1 - \Psi & \Psi \end{bmatrix}. \qquad (4)$$

To verify the ability of the DTMC model of (4) to reproduce the DC of real channels, the empirical data captured in the measurement campaign were used to estimate the transition probabilities of each channel as

$$\hat{p}_{ij} = \begin{cases} \frac{\eta_{ij}}{\eta_i}, & \eta_i > 0 \\ 0, & \eta_i = 0 \text{ and } i = j \\ 1, & \eta_i = 0 \text{ and } i \neq j \end{cases} \qquad (5)$$

where η_{ij} represents the number of transitions from state s_i to s_j occurring in the empirical sequences, and $\eta_i = \sum_{k=0}^{n-1} \eta_{ik}$ is the number of times that the channel resides in state s_i. The two last cases of (5) are included to account for channels that are always busy ($\Psi = 1$) or always idle ($\Psi = 0$). The theoretical DC corresponding to the estimated probabilities $\hat{p}_{ij}$ was estimated based on (3) and compared with the true empirical DC of the channel, appreciating a perfect agreement for channels of all the considered radio technologies. This indicates that the DTMC model of (4) is able to accurately reproduce the DC of real channels.[5]

Nevertheless, reproducing not only the DC but the lengths of the busy and idle periods as well is an important characteristic of a realistic time-dimension model of spectrum use. While this feature is explicitly represented in the case of CTMC and CTSMC models by means of the sojourn time distributions, there is no mean to account for the state holding times in the case of the DTMC model. Therefore, the DTMC model would not be expected to reproduce the statistical properties of the lengths of busy and idle periods of real channels. To verify this statement, the DTMC channel model was simulated with the transition probabilities $\hat{p}_{ij}$ estimated from empirical data for all the measured channels. During the simulation of the DTMC model, the durations of state holding times T_i were computed as $T_i = \tilde{\eta}_i \cdot T_s$, where $\tilde{\eta}_i$ represents the number of consecutive steps the channel resides in state s_i during the simulation before switching to the other state, and T_s is the average sweep time corresponding to the considered channel (see Table I). The statistical distributions of busy and idle periods obtained by means of simulation were computed and compared with the empirical
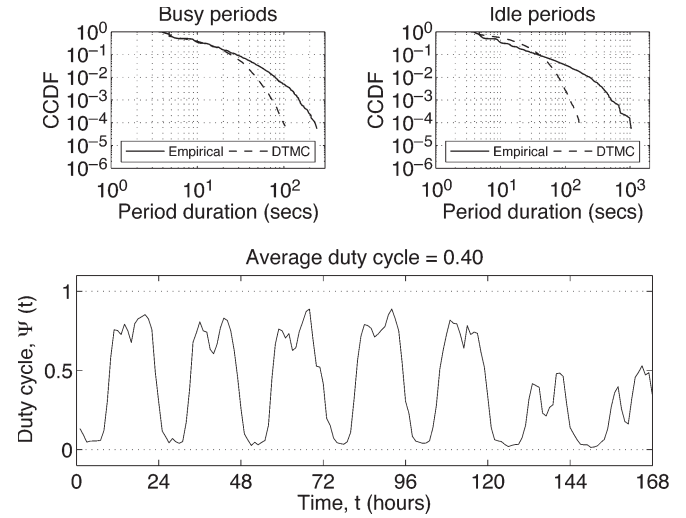

Fig. 3. Empirical and DTMC-simulated distributions of busy and idle periods along with DC time evolution for DCS 1800 downlink (DL) channel 70.
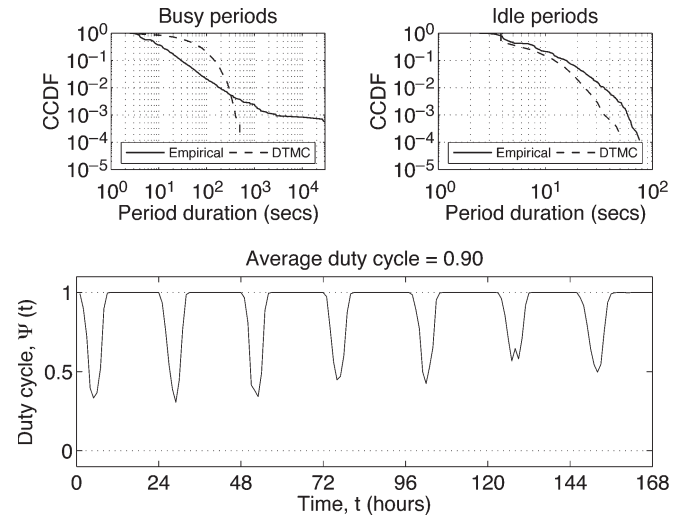

Fig. 4. Empirical and DTMC-simulated distributions of busy and idle periods along with DC time evolution for E-GSM 900 DL channel 23.

distributions of busy and idle periods observed in the measured channels. This comparison was performed for each measured channel of every radio technology. Figs. 3–6 show the results obtained for some selected channels. The results are shown in terms of the complementary cumulative distribution function and with axes in logarithmic scale for a finer detail of accuracy. The time evolution of the DC computed over 1-h periods is also shown. In general, the obtained results indicate, as expected, that the DTMC channel model is not able to reproduce the statistical properties of the lengths of busy and idle periods of real channels. In some cases, however, the distributions resulting from simulations showed a noticeable agreement with their empirical counterparts (Fig. 6 shows an example). After analyzing the empirical data in detail, it was observed that the convergence/divergence of empirical and simulation results can be explained in terms of the channel load variation pattern. When the channel is sparsely used (low load), the length of idle periods is significantly higher than that of busy periods. On the other hand, when the channel is subject to an intensive usage

---

[5]For CTMC and CTSMC models, any arbitrary DC can be also reproduced by appropriately selecting the parameters of the sojourn time distributions to provide mean values $\mathbb{E}\{T_i\}$ such that $\Psi = \mathbb{E}\{T_1\}/(\mathbb{E}\{T_0\} + \mathbb{E}\{T_1\})$ [66], where $\mathbb{E}\{T_0\}$ and $\mathbb{E}\{T_1\}$ are the mean sojourn times in the idle and busy states, respectively.
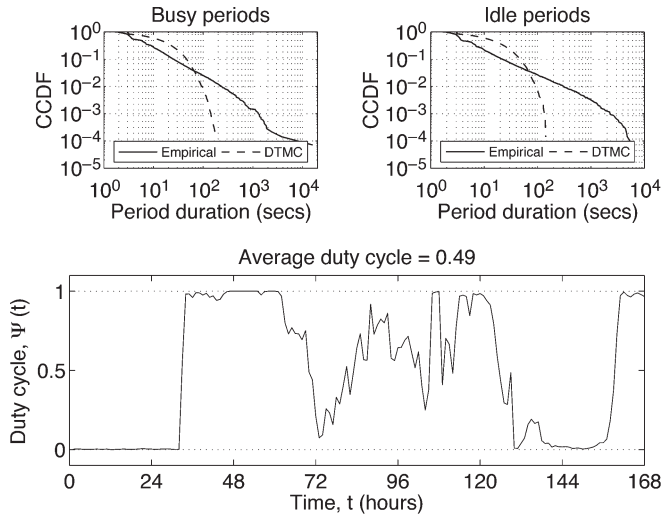
Fig. 5.   Empirical and DTMC-simulated distributions of busy and idle periods along with DC time evolution for TETRA DL channel 340.
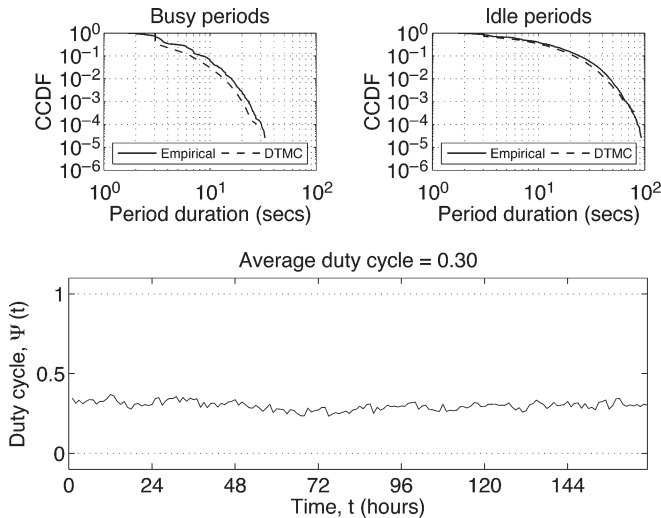

Fig. 6.   Empirical and DTMC-simulated distributions of busy and idle periods along with DC time evolution for TETRA uplink channel 375.

(high load), the length of busy periods increases, whereas idle periods become notably shorter. Since the considered DTMC model is parameterized (i.e., the transition probabilities are configured) based on the long-term average load of the channel (i.e., the average DC of the whole measurement period), it is not able to capture the channel load variations, and as a result, the DTMC model cannot reproduce the resulting lengths of busy and idle periods. This can clearly be appreciated in Figs. 3–5, where the channel load, which is characterized in terms of the DC, varies with the time and the distributions obtained by simulation diverge from the real distributions. The exception, however, corresponds to the case of channels with constant load patterns, where the average DC matches the *instantaneous* DC at all times, and simulation and empirical results then agree, as shown in Fig. 6.

Since the probabilities of transition matrix $\mathbf{P}$ depend on the DC Ψ, and Ψ changes over time, this means that the binary occupancy pattern of real channels cannot be modeled, in gen-

eral, by means of a stationary (time-homogeneous) DTMC[6] as widely considered in DSA/CR research (see Section II-B). As a result, a nonstationary (time-inhomogeneous) DTMC should be considered with a time-dependent transition matrix

$$\mathbf{P}(t) = \begin{bmatrix} 1 - \Psi(t) & \Psi(t) \\ 1 - \Psi(t) & \Psi(t) \end{bmatrix} \qquad (6)$$

where $t = t_k = kT_s$, as previously defined.

In the stationary case of (4), Ψ represents a constant parameter. However, in the nonstationary case of (6), $\Psi(t)$ represents a time-dependent function that needs to be characterized to characterize the DTMC channel model in the time domain. Appropriate and accurate DC models for $\Psi(t)$ are therefore required.

The results derived from the empirical data indicated the existence of two well-defined types of channel load variation patterns, namely, patterns with an important and remarkably predominant deterministic component (e.g., see Figs. 3 and 4) and patterns where the carried load appears to vary following a random behavior (e.g., see Fig. 5). Based on this observation, adequate DC models of $\Psi(t)$ for both cases are developed in Sections V and VI, following deterministic and stochastic modeling approaches, respectively.

V. DETERMINISTIC DUTY CYCLE MODEL

In many interesting and important cases, the load variation pattern of primary radio channels is characterized by a predominant deterministic component arising from social behavior and common habits, as can clearly be appreciated in Figs. 3 and 4. These examples correspond to cellular mobile communication systems, namely, E-GSM 900 and DCS 1800. Nevertheless, it is interesting to note that similar patterns were also observed in some channels from other radio technologies such as TETRA. Moreover, deterministic patterns with different shapes were also identified in other cases. This section focuses on the analysis and modeling of the spectrum occupancy patterns commonly observed in cellular mobile communication systems, which are a clear example of predominantly deterministic behaviors. The same modeling approach can be used and extended to represent other particular patterns that may be found in practice.

The load variation pattern of a cellular system was studied in [67] by means of time-series analysis and autoregressive integrated moving average models. Here, however, an alternative approach is developed based on the observation that the time evolution of $\Psi(t)$ over time periods of certain length exhibits a clear and predominant deterministic component. Moreover, the analysis of the empirical data corresponding to E-GSM 900 and DCS 1800 indicated that the variation pattern of $\Psi(t)$ is periodic with a period of one day and a slightly different shape between weekdays and weekends due to the lower traffic load normally associated with weekends. Two different shape types for $\Psi(t)$ were identified in the empirical data. The first shape

---

[6]A stationary DTMC may be appropriate for a limited time period only if the modeled system shows approximately stationary behavior during this period. Otherwise, a nonstationary DTMC modeling approach is necessary.
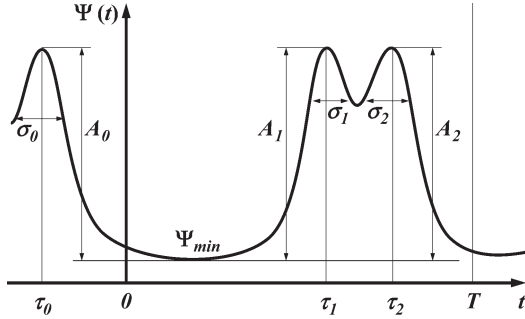
Fig. 7. Parameters of the deterministic DC model for low/medium loads.

type was normally observed in channels with low/medium loads (average DCs) as in the example in Fig. 3, whereas the second shape type was more frequently observed in channels with medium/high loads, as is the case in Fig. 4. Similar patterns were observed in [68].

A. Deterministic DC Model for Low/Medium Loads

The shape of $\Psi(t)$ in this case can be approximated by the summation of M bell-shaped exponential terms centered at time instants τ_m, with amplitudes A_m and widths σ_m, i.e.,

$$\Psi(t) \approx \Psi_{min} + \sum_{m=0}^{M-1} A_m e^{-\left(\frac{t-\tau_m}{\sigma_m}\right)^2}, \qquad 0 \leq t \leq T \quad (7)$$

where $\Psi_{\min} = \min\{\Psi(t)\}$, and T is the time interval over which $\Psi(t)$ is periodic (i.e., one day). The analysis of empirical data indicated that $\Psi(t)$ can be accurately described by means of $M = 3$ terms, with τ_1 and τ_2 corresponding to *busy hours* and $\tau_0 = \tau_2 - T$, as shown in Fig. 7.

Based on empirical results, approximations $A_0 = A_1 = A_2 = A$ and $\sigma_0 = \sigma_1 = \sigma_2 = \sigma$ are acceptable without incurring in excessive errors, which simplifies the model. Notice that A determines the average value of $\Psi(t)$ in the time interval $[0, T]$, which is denoted by $\overline{\Psi}$, and it can be therefore expressed as a function of $\overline{\Psi}$ taking into account that

$$\overline{\Psi} = \frac{1}{T} \int_0^T \Psi(t) dt \approx \Psi_{\min} + \frac{A}{T} \sum_{m=0}^{M-1} \int_0^T e^{-\left(\frac{t-\tau_m}{\sigma}\right)^2} dt. \quad (8)$$

Solving (8) for A and substituting in (7) yields

$$\Psi(t) \approx \Psi_{\min} + \frac{2T(\overline{\Psi} - \Psi_{\min})}{\sigma\sqrt{\pi}} \cdot \frac{f_{\exp}^{l/m}(t, \tau_m, \sigma)}{f_{\mathrm{erf}}^{l/m}(T, \tau_m, \sigma)} \quad (9)$$

where $\overline{\Psi} \geq \Psi_{\min}$, and

$$f_{\exp}^{l/m}(t, \tau_m, \sigma) = \sum_{m=0}^{M-1} e^{-\left(\frac{t-\tau_m}{\sigma}\right)^2} \quad (10)$$

$$f_{\mathrm{erf}}^{l/m}(T, \tau_m, \sigma) = \sum_{m=0}^{M-1} \left[\mathrm{erf}\left(\frac{\tau_m}{\sigma}\right) + \mathrm{erf}\left(\frac{T-\tau_m}{\sigma}\right) \right]. \quad (11)$$

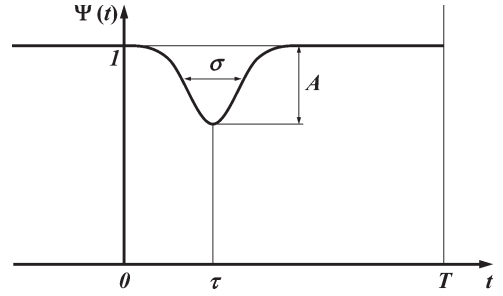Equations (9)–(11) constitute the empirical DC model of $\Psi(t)$ for low/medium loads.

Fig. 8. Parameters of the deterministic DC model for medium/high loads.

B. Deterministic DC Model for Medium/High Loads

The shape of $\Psi(t)$ in this case can be approximated by an expression based on a single bell-shaped exponential term centered at time instant τ, with amplitude A and width σ, i.e.,

$$\Psi(t) \approx 1 - A e^{-\left(\frac{t-\tau}{\sigma}\right)^2}, \qquad 0 \leq t \leq T \quad (12)$$

where T is the time interval over which $\Psi(t)$ is periodic (i.e., one day). The model is illustrated in Fig. 8, with τ corresponding to the hour with the lowest activity levels.

As in the previous case, A determines the average value of $\Psi(t)$ in the time interval $[0, T]$, and it can be therefore expressed as a function of $\overline{\Psi}$ taking into account that

$$\overline{\Psi} = \frac{1}{T} \int_0^T \Psi(t) dt \approx 1 - \frac{A}{T} \int_0^T e^{-\left(\frac{t-\tau}{\sigma}\right)^2} dt. \quad (13)$$

Solving (13) for A and substituting in (12) yields

$$\Psi(t) \approx 1 - \frac{2T(1 - \overline{\Psi})}{\sigma\sqrt{\pi}} \cdot \frac{f_{\exp}^{m/h}(t, \tau, \sigma)}{f_{\mathrm{erf}}^{m/h}(T, \tau, \sigma)} \quad (14)$$

where

$$f_{\exp}^{m/h}(t, \tau, \sigma) = e^{-\left(\frac{t-\tau}{\sigma}\right)^2} \quad (15)$$

$$f_{\mathrm{erf}}^{m/h}(T, \tau, \sigma) = \mathrm{erf}\left(\frac{\tau}{\sigma}\right) + \mathrm{erf}\left(\frac{T-\tau}{\sigma}\right). \quad (16)$$

Equations (14)–(16) constitute the empirical DC model of $\Psi(t)$ for medium/high loads.

C. Deterministic DC Model Validation and Applicability

The objective of this section is to evaluate the ability of the DC models in Sections V-A and B to describe the time evolution of $\Psi(t)$ with sufficient accuracy. To this end, the empirical values of $\Psi(t)$ were averaged among 24-h periods of the same category (i.e., weekdays and weekends) to reduce the unavoidable random component of empirical data and extract the deterministic component. The mathematical expressions of (9)–(11) and (14)–(16) were then fitted to the empirical data by means of curve-fitting procedures. The results are shown in Figs. 9 and 10, indicating that the proposed DC models are able to accurately reproduce the deterministic component of $\Psi(t)$ in real-world channels.

To facilitate researchers in the application of the models in analytical studies and simulations, realistic values of the
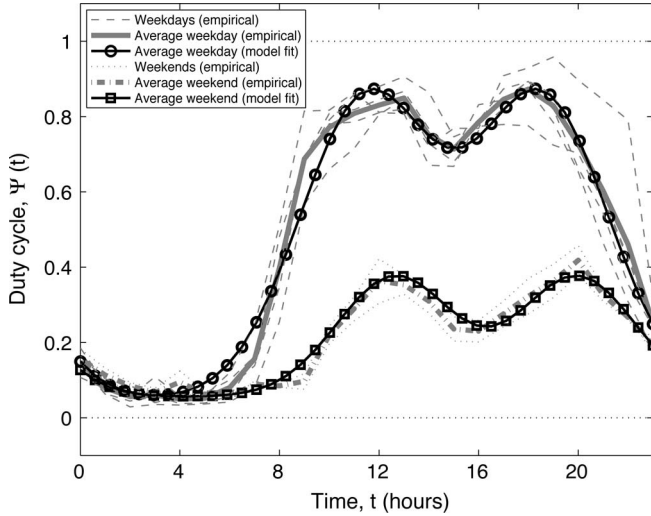
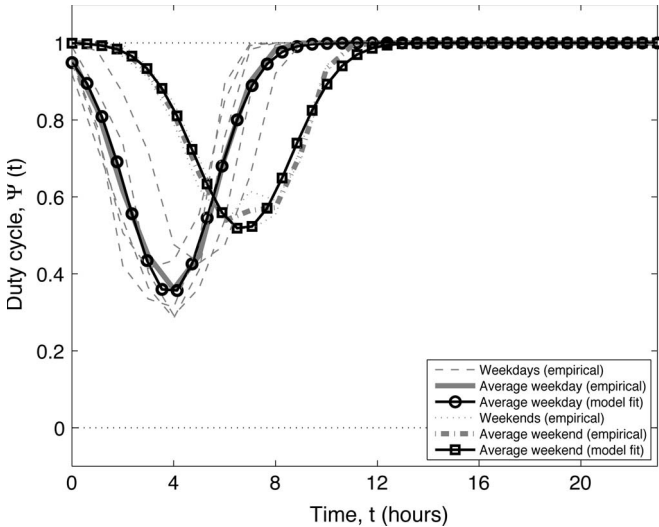Fig. 9. Validation of the deterministic DC model for low/medium loads.

Fig. 10. Validation of the deterministic DC model for medium/high loads.

models' parameters were estimated based on the empirical measurements and by means of curve-fitting procedures. The fitted results are shown in Table II. The values are specified in "(minimum; average; maximum)" format. In addition to the models' parameters, the parameter

$$\kappa = \frac{\overline{\Psi}_{\text{weekends}}}{\overline{\Psi}_{\text{weekdays}}} \qquad (17)$$

has also been included to characterize the load level differences observed between weekdays and weekends.

Notice that $\overline{\Psi}$ has not been specified in Table II since this parameter is assumed to be a variable that can be configured to reproduce the shape of $\Psi(t)$ with any arbitrary mean $\overline{\Psi}$. With regard to this aspect, it is important to mention that, based on the captured empirical data, it was observed that the DC model for low/medium loads is valid from $\overline{\Psi} = 0$ to $\overline{\Psi} \approx 0.60/0.70$. The maximum $\overline{\Psi}$ for which the model is valid depends on the particular set of selected parameters. For the average values

TABLE II
FITTED VALUES OF THE DETERMINISTIC DC MODEL PARAMETERS

Load	Parameter	Weekdays	Weekends
Low/ /Med	Ψ_{min}	(0.00; 0.04; 0.31)	(0.00; 0.05; 0.35)
	τ_1 (hours)	(10.74; 11.65; 12.28)	(12.04; 13.03; 14.05)
	τ_2 (hours)	(17.80; 18.99; 20.09)	(19.28; 20.42; 21.54)
	σ (hours)	(3.00; 3.88; 4.31)	(2.49; 3.59; 5.83)
	κ	(0.18; 0.51; 0.82)	
Med/ /High	τ (hours)	(2.94; 3.65; 4.08)	(5.64; 6.44; 7.82)
	σ (hours)	(1.99; 2.81; 6.03)	(2.29; 3.41; 8.00)
	κ	(0.69; 0.97; 1.00)	

of the fitted parameters in Table II, the model is valid up to $\overline{\Psi} = 0.58$ for weekdays and $\overline{\Psi} = 0.55$ for weekends. On the other hand, the DC model for medium/high loads is valid from $\overline{\Psi} \approx 0.46/0.85$ to $\overline{\Psi} = 1$. Again, the minimum $\overline{\Psi}$ for which the model is valid depends on the particular set of selected parameters. For the average values in Table II, the model is valid down to $\overline{\Psi} = 0.80$ for weekdays and $\overline{\Psi} = 0.75$ for weekends. Invalid configurations can be readily identified since, in these cases, $\Psi(t)$ surpasses the interval $[0, 1]$ within which it must be mandatorily confined.

It is worth noting that the values shown in Table II correspond to empirical measurements performed at a particular location and, as such, are unavoidably affected by the local habits. For example, the usual lunchtime in Spain is around 2:00 P.M., and it takes place within a lunch break of a couple of hours. This schedule may be usually delayed about 1 h on weekends. This behavior is indeed clearly appreciated in Fig. 9. Habits may be different in other countries (e.g., see [69, Fig. 2] and [70, Fig. 4]), which may result in distinct shapes for $\Psi(t)$. The DC models of (9)–(11) and (14)–(16) can be still valid by fitting the mathematical equations to different empirical data. For instance, an earlier lunchtime would result in a lower value of τ_1, whereas a shorter lunch break (if any) would result in τ_1 and τ_2 being closer to each other. The DC models, nevertheless, would still be valid.

Finally, the DC models in Sections V-A and -B are envisaged to reproduce the deterministic pattern normally observed in cellular mobile communication systems such as E-GSM 900 and DCS 1800, which may be also present in other systems. Nevertheless, this does not imply that the model is always applicable to such type of systems. For instance, if the system is studied over a relatively short time period (e.g., a few hours), social behavior and external events, which may not be easily predicted, may have a significant short-term impact on channel usage. This may cause the deterministic component of $\Psi(t)$ to loss importance with respect to the random component, and as a result, the occupancy of a single channel may experience high and unpredictable variations (e.g., see [71]). In such a case, deterministic DC models may be no longer valid, and stochastic modeling approaches, such as those discussed in Section VI, might be a more appropriate alternative.

VI. STOCHASTIC DUTY CYCLE MODEL

The traffic load experienced in a radio channel is normally the consequence of a significant number of random factors such as the number of incoming and outgoing users, the resource
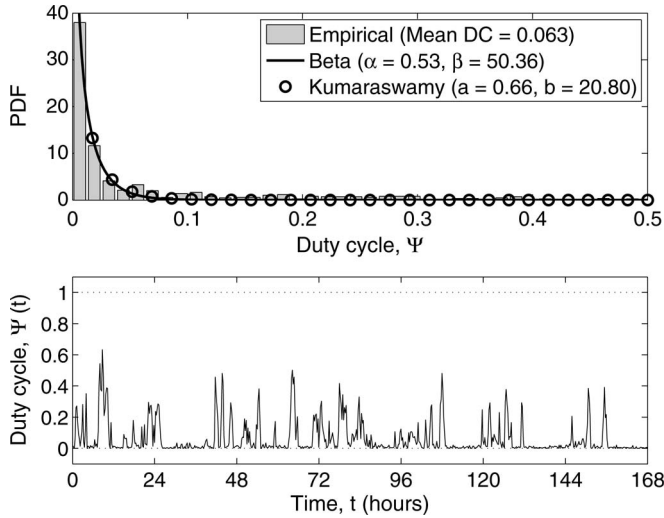
Fig. 11. Stochastic DC models. Case L.I.

Fig. 12. Stochastic DC models. Case M.I.

management policies employed in the system, and so forth. As a result, the channel usage level, which is represented by means of $\Psi(t)$, is itself a random variable (see the example in Fig. 5). In such a case, a stochastic modeling perspective appears to be a more convenient approach.

The following discussion assumes ergodicity on $\Psi(t)$, meaning that the expected values of its moments, such as its mean and variance, can be estimated as the time averages of the moments, which can be computed from a single sample (i.e., realization) of the process provided that it is sufficiently long. Notice that the sequence of $\Psi(t)$ values empirically derived from the measurements for a given channel represents a single realization of the underlying stochastic process, which is not enough to draw any conclusions on its ergodicity. Nevertheless, as it will be shown later on, the model developed under this assumption results valid and accurate in practice.

To determine the statistical properties of the underlying stochastic process based on the captured empirical data, $\Psi(t)$ was obtained for each channel as the time evolution of the DC computed over periods of various lengths, ranging from a few minutes up to 1 h. Assuming ergodicity, the probability density function (pdf) of the underlying stochastic process can be estimated as the empirical pdf resulting from the empirical $\Psi(t)$ values for the considered channel. The empirical pdf's obtained with this procedure were compared with various bounded pdf models. Based on curve-fitting procedures, it was found that the empirical pdf's of $\Psi(t)$ can be accurately fitted with the beta distribution [72] and the Kumaraswamy distribution [73], as can be appreciated in the examples in Figs. 11–16. The pdf for the former is given by

$$f_x^B(x; \alpha, \beta) = \frac{1}{B(\alpha, \beta)} x^{\alpha-1} (1-x)^{\beta-1}, \qquad x \in (0, 1) \tag{18}$$

where $\alpha > 0$ and $\beta > 0$ are shape parameters, and $B(\alpha, \beta)$ is the beta function given by [74, 6.2.1]

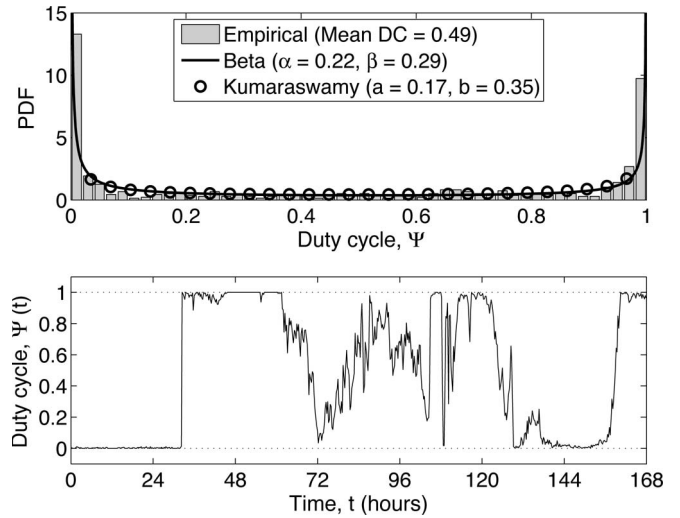$$B(\alpha, \beta) = \int_0^1 z^{\alpha-1} (1-z)^{\beta-1} dz \tag{19}$$
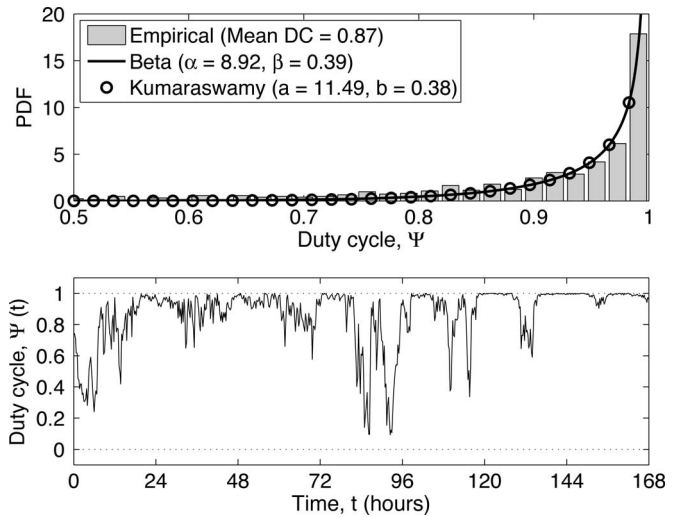

Fig. 13. Stochastic DC models. Case H.I.

whereas the pdf for the latter is given by

$$f_x^K(x; a, b) = abx^{a-1}(1-x^a)^{b-1}, \qquad x \in (0, 1) \tag{20}$$

where $a > 0$ and $b > 0$ are shape parameters.

The beta distribution is a well-known and widely used distribution that can be found in many popular software simulation packages, thus facilitating the implementation of the stochastic DC model in simulation tools. However, it might present some difficulties in analytical studies due to the complex expression of its pdf. The Kumaraswamy distribution is similar to the beta distribution but much simpler to use in analytical studies due to the simpler closed form of its pdf [75]. Therefore, whereas the former may be more appropriate for simulations, the latter may be more convenient for analytical studies.

Both distributions can be configured to reproduce any arbitrary mean DC, i.e., $\overline{\Psi}$, by properly selecting the distribution's parameters. In particular, the mean value of the beta
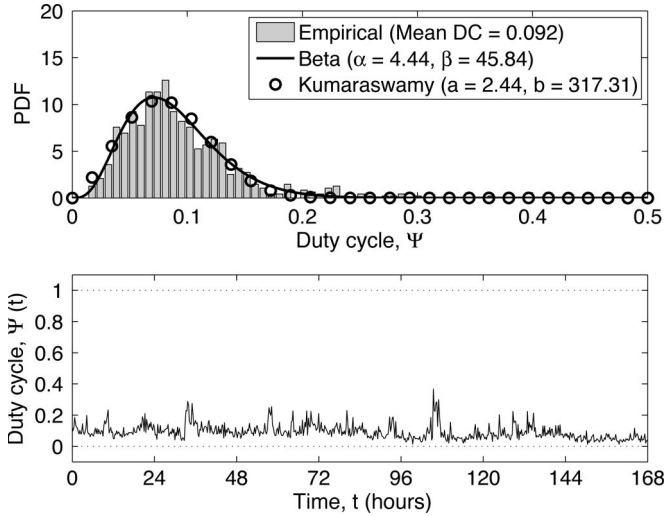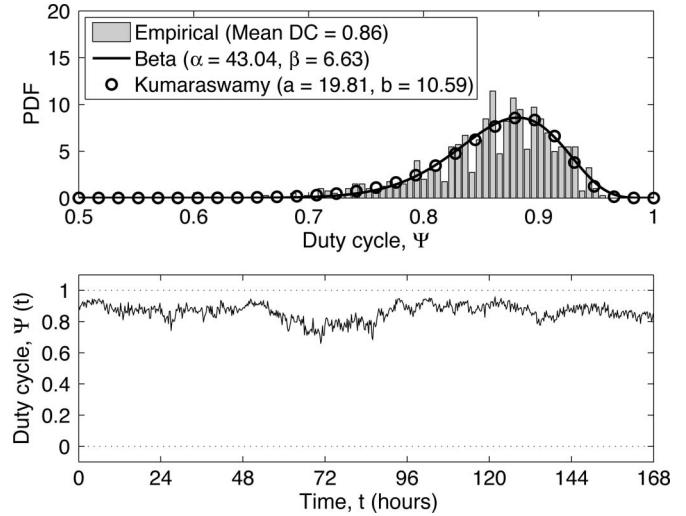
Fig. 14. Stochastic DC models. Case L.II.

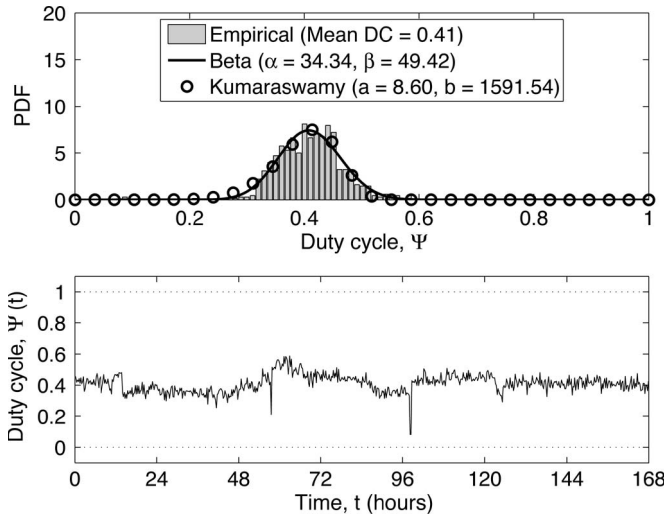Fig. 15. Stochastic DC models. Case M.II.

Fig. 16. Stochastic DC models. Case H.II.

and Kumaraswamy distributions are related with their shape parameters as [72], [73]

$$\overline{\Psi} = \frac{\alpha}{\alpha + \beta} = bB\left(1 + \frac{1}{a}, b\right). \tag{21}$$

Notice that (21) can be satisfied for a given $\overline{\Psi}$ with different combinations of shape parameters α, β and a, b. The particular selection of the shape parameters determines the resulting shape of the distributions. To facilitate researchers in the application of the models and their configuration, an exhaustive analysis of the empirical data was performed to identify any potential relation between the shape parameters and the resulting channel occupancy pattern in the time domain. Based on such analysis, it was found that the pdf shapes observed in real channels can be classified into six elemental archetypes, each with a characteristic time-domain pattern. Each archetype is defined by its load level (L: low; M: medium; H: high), as well as its load pattern (type I: very bursty; type II: moderately bursty but not constant). The range of shape parameters for each

archetype and the corresponding time-domain pattern are given here (see Figs. 11–16).

1) Case L.I ($\alpha < 1, \beta \geq 1$): The channel is sporadically used ($\Psi(t) > 0$) and remains unused ($\Psi(t) \approx 0$) most of the time.
2) Case L.II ($1 < \alpha < \beta$): The channel is regularly used ($\Psi(t) > 0$) by traffic with low activity factors.
3) Case M.I ($\alpha < 1, \beta < 1$): The channel is subject to an intermittent use, where high-load periods are followed by low-load periods in a similar proportion.
4) Case M.II ($\alpha > 1, \beta > 1, \alpha \sim \beta$): The channel usage level weakly oscillates around the average level.
5) Case H.I ($\alpha \geq 1, \beta < 1$): The channel is used ($\Psi(t) \approx 1$) most of the time, with some periods of lower occupancy levels ($\Psi(t) < 1$).
6) Case H.II ($\alpha > \beta > 1$): The channel is not fully used ($\Psi(t) < 1$) but subject to a constant intensive usage.

The range of values indicated for the parameters of the beta distribution is also valid for the Kumaraswamy distribution by replacing α with a and β with b in type-I cases. In type-II cases, the resulting Kumaraswamy distribution is more difficult to control since the same constraints on a and b may hold for various load levels. Based on the aforementioned archetypes and the corresponding range of shape parameters, along with (21), the parameters of the models can be configured to reproduce not only arbitrary mean load levels but various occupancy patterns observed in real channels as well.

VII. MODEL VALIDATION

The aim of this section is to assess the ability of the overall model, which is composed of the DTMC along with the deterministic and stochastic DC models, to reproduce with sufficient accuracy not only the mean DC of the channel but the statistical properties of the busy and idle periods as well.

To this end, the DTMC model in Fig. 2 was simulated for a sufficiently high number of iterations (transitions), and at different iterations during the simulation, transition matrix $\mathbf{P}(t)$
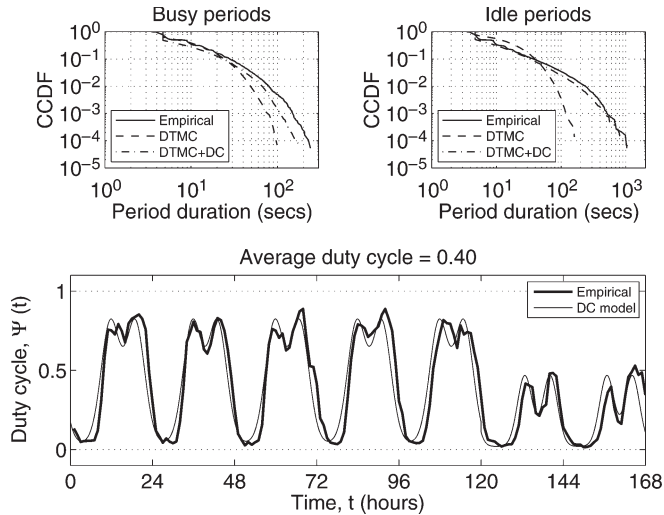
Fig. 17. Empirical and DTMC-simulated distributions of busy and idle periods along with DC time evolution for DCS 1800 DL channel 70.
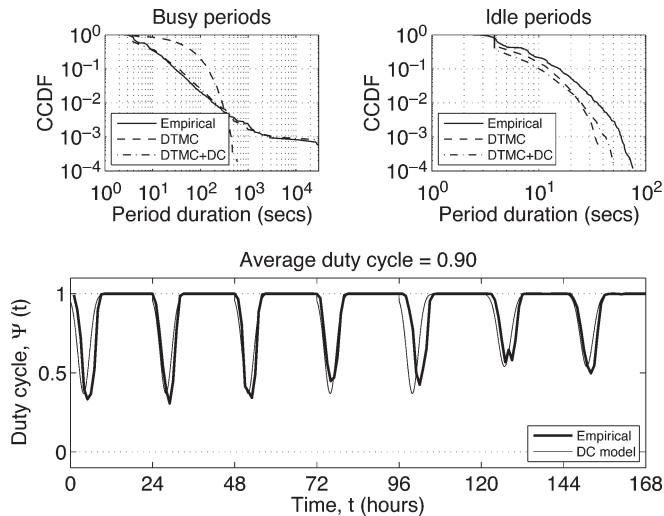

Fig. 18. Empirical and DTMC-simulated distributions of busy and idle periods along with DC time evolution for E-GSM 900 DL channel 23.

[see (6)] was updated based on the DC models in Sections V and VI. In the deterministic case, $\Psi(t)$ is computed based on (9) and (14) and taking into account the simulation time instant. In the stochastic case, $\Psi(t)$ is drawn from a beta distribution whose parameters are estimated based on the sample mean and the sample variance of the empirical $\Psi(t)$. The stationary case widely considered in previous DSA/CR research [see (4)], where the DC is fixed and equal to the mean value, i.e., $\Psi(t) = \overline{\Psi} \ \forall t$, was also simulated. The statistical distributions obtained in both cases were compared with the real distributions derived from empirical data. The obtained results are shown in Figs. 17–19.

As it can be appreciated in Figs. 17 and 18, the deterministic DC models are able to closely follow and reproduce the deterministic component of $\Psi(t)$ in the time domain, and as a result, the overall model is able to reproduce not only the mean DC of the channel, i.e., $\overline{\Psi}$, but the statistical properties of busy and idle periods as well, which does not occur with the stationary
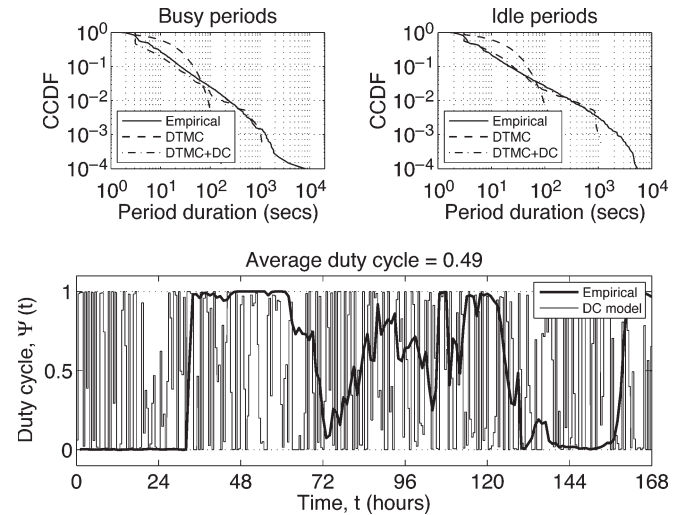

Fig. 19. Empirical and DTMC-simulated distributions of busy and idle periods along with DC time evolution for TETRA DL channel 340.

case where the DTMC is simulated without appropriate DC models.

In the case of the stochastic DC model, the generated sequence of $\Psi(t)$ values does not follow the empirical $\Psi(t)$ values of the channel in the time domain, as it can be appreciated in Fig. 19. However, it is important to note that the stochastic approach is not aimed at reproducing the time evolution of a particular realization of the stochastic process $\Psi(t)$ but the statistical properties thereof. The results shown in Fig. 19 demonstrate that this modeling approach is also a valid and significantly accurate alternative to reproduce the statistical properties of busy and idle periods of real channels.

Taking into account the logarithmic axis representation in Figs. 17–19, it can be appreciated that the distributions of busy and idle periods are reproduced with a significant level of precision. To objectively assess the accuracy, the Kolmogorov–Smirnov (KS) test [76] was performed over the obtained simulation results to compute the KS distances $D_{KS}(T_0)$ and $D_{KS}(T_1)$, for idle and busy periods, respectively, between the empirical distribution functions and the corresponding counterparts obtained by means of simulation. Such study indicated that $D_{KS}(T_0) = 0.08$ and $D_{KS}(T_1) = 0.09$ (in Fig. 17) and $D_{KS}(T_0) = 0.13$ and $D_{KS}(T_1) = 0.06$ (in Fig. 18), whereas $D_{KS}(T_0) = 0.06$ and $D_{KS}(T_1) = 0.09$ (in Fig. 19), which highlights the remarkably good accuracy of the proposed modeling approach.

Before concluding this section, it is worth noting that the practical implementation of the stochastic DC model in simulation tools may not lead to accurate results if some observations are not carefully taken into account. In particular, the DTMC has to be iterated a sufficient number of times N before updating $\mathbf{P}(t)$ according to the stochastic DC model. During such numbers of iterations, the transition probabilities of the DTMC must remain unaltered. After such N iterations, a new value of $\Psi(t)$ can be generated from a beta or a Kumaraswamy distribution and used to update transition matrix $\mathbf{P}(t)$ for the next N iterations. If the transition matrix is updated excessively fast (e.g., every iteration), the overall model may not be able to accurately reproduce the lengths of busy and idle periods.
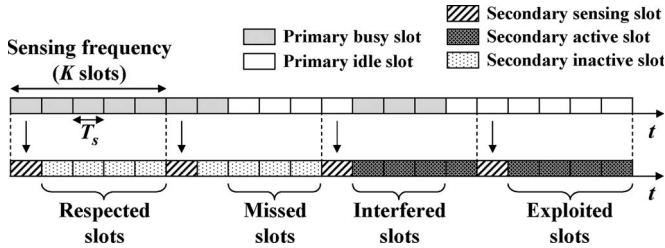
Fig. 20. Case study description.

In conclusion, the obtained results demonstrate that the non-stationary DTMC model along with the proposed deterministic and stochastic DC models is able to accurately reproduce not only the mean occupancy but the statistical properties of busy and idle periods observed in real channels as well.

VIII. CASE STUDY

The aim of this section is to demonstrate and illustrate the importance of employing realistic and accurate spectrum occupancy models in the design and evaluation of DSA/CR techniques. To this end, this section considers a simple medium-access scheme where a CR terminal senses a primary radio channel periodically and accesses the channel whenever it is sensed as idle. Although the case study of this section may be considered to be trivial, it will suffice to illustrate the impact of the realism and accuracy of spectrum occupancy models on the design and performance evaluation of more sophisticated solutions such as adaptive spectrum-sensing techniques, MAC protocols, MAC-layer sensing schemes, dynamic channel selection algorithms, and opportunistic scheduling policies.

Let us assume that the CR terminal senses and accesses the channel on a frame basis, as shown in Fig. 20. Each frame is composed of K slots with duration T_s. The CR terminal senses the channel in the first slot of the frame and decides to transmit or not in the following $K - 1$ slots based on the sensing result (perfect sensing is assumed). If the CR terminal senses the channel as busy and decides not to transmit, the following slots may be classified as *respected slots* if the primary user transmits in such slots or *missed slots* otherwise. On the other hand, a secondary transmission may result in *interfered slots* if the primary is also active, or *exploited slots* otherwise, as shown in Fig. 20.

The objective is to evaluate the performance of the considered medium-access scheme when the sequence of channel occupancy states corresponds to the following: 1) empirical measurements of real channels; 2) occupancy sequences generated with the nonstationary DTMC model along with DC models; and 3) occupancy sequences generated with the stationary DTMC model alone. The comparison of the results obtained in these cases will provide a quantitative illustration of the consequences of considering (un)realistic and (in)accurate spectrum occupancy models in DSA/CR research.

Table III shows the channel access statistics obtained for the aforementioned sequences of channel occupancy states in the case of a DECT channel. As it can be appreciated, the proposed nonstationary approach (labeled "DTMC + DC")

TABLE III
CHANNEL ACCESS STATISTICS FOR DECT CHANNEL 9
(STOCHASTIC DC MODEL AND $K = 5$)

Slot type	Empirical	DTMC+DC	DTMC
Respected	2.67%	2.75%	1.16%
Missed	8.34%	8.31%	9.95%
Interfered	8.25%	8.30%	9.73%
Exploited	80.74%	80.64%	79.16%

TABLE IV
CHANNEL ACCESS STATISTICS FOR TETRA DL CHANNEL 340
(STOCHASTIC DC MODEL AND $K = 5$)

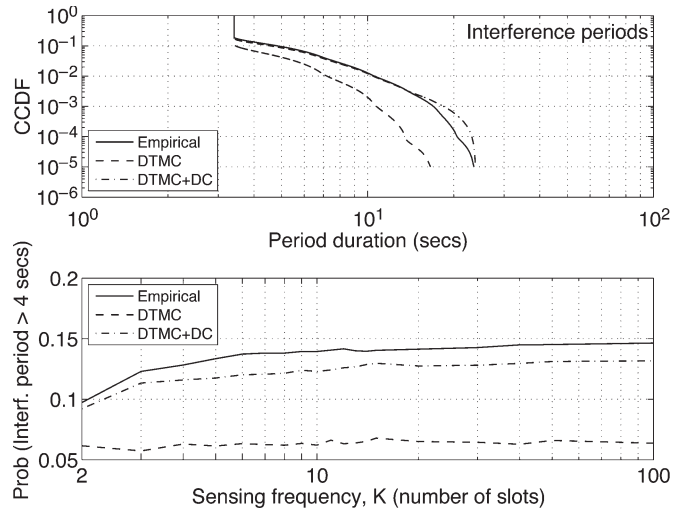| Slot type	Empirical	DTMC+DC	DTMC
Respected	41.37%	41.15%	23.84%
Missed	7.39%	7.23%	25.25%
Interfered	7.20%	7.81%	24.72%
Exploited	44.04%	43.81%	26.19%

Fig. 21. Interference results for DECT channel 9. (Top) Distribution of interference periods ($K = 5$). (Bottom) Probability of interference as a function of the sensing frequency ($\delta_d = 4$ s).

is able to provide accurate estimations of the true channel use statistics. The results provided by the stationary approach (labeled "DTMC"), although less accurate, can be considered acceptable as well. This can be explained by the fact that the considered metrics represent the average number of slots for each type in the long term. As such, they depend on the average number of busy/idle slots or, in other words, the average DC of the channel. Since both DTMC modeling alternatives (stationary and nonstationary) are able to accurately reproduce the channel's average DC, the obtained average values for the considered metrics agree in both cases with the empirical real data. However, it is worth noting that, in M.I-type channels (referring to the nomenclature used in Section VI), the stationary DTMC model was observed to fail in providing acceptable results, whereas the proposed nonstationary DTMC model was still able to do so, as shown in Table IV. Therefore, although the stationary DTMC model is able to reproduce the true mean DC value of the channel, this does not guarantee the reliability of average performance metrics obtained when applying such model. On the other hand, the proposed nonstationary DTMC

approach provides accurate estimates of average performance metrics.

The average value of performance metrics, although useful, may not provide a full impression on the real performance of a DSA/CR technique under study. For example, let us assume that a primary user tolerates a short communication disruption provided that its duration is below a given threshold δ_d. In such a case, the probability that the duration of interference periods exceeds δ_d would be a more useful performance metric than the average number of interfered slots. As shown in Fig. 21, the distribution of interference periods resulting from the medium-access technique under study is accurately reproduced by the proposed nonstationary DTMC modeling approach, which is not the case of the stationary DTMC model. As a result, the real interference to a primary user is accurately estimated with the former, whereas it is significantly underestimated with the latter. Concretely, while the application of the stationary DTMC model results in errors up to 9% in the predicted interference probability, the prediction provided by the proposed nonstationary DTMC model is around 1% below the real value obtained from the real channel occupancy pattern. Therefore, even when the stationary DTMC approach is able to provide accurate estimates of average metrics, it fails in providing acceptable results for other more sophisticated performance metrics. These results demonstrate and highlight the importance of employing realistic and accurate spectrum occupancy models, such as those proposed in this paper, for the design and performance evaluation of DSA/CR techniques.

IX. CONCLUSION

Due to the opportunistic nature of the DSA/CR principle, the behavior and performance of a secondary network depends on the spectrum occupancy patterns of the primary system. A realistic and accurate modeling of such patterns therefore becomes essential. This paper has demonstrated that the stationary DTMC model widely used in the DSA/CR literature to describe the binary occupancy pattern of primary channels in the time domain is not able to reproduce relevant properties of spectrum use. As a result, a nonstationary DTMC model with deterministic and stochastic DC models has been developed. The proposed approach has been validated with extensive empirical measurement results, demonstrating that it is able to accurately reproduce not only the mean occupancy level but the statistical properties of busy and idle periods observed in real-world channels as well. The importance of realistically and accurately modeling spectrum use in the design and evaluation of DSA/CR techniques has been highlighted with a practical case study.

REFERENCES

[1] M. A. McHenry *et al.*, Spectrum occupancy measurements, Shared Spectrum Company, Vienna, VA. [Online]. Available: http://www.sharedspectrum.com

[2] A. Petrin and P. G. Steffes, "Analysis and comparison of spectrum measurements performed in urban and rural areas to determine the total amount of spectrum usage," in *Proc. ISART*, Mar. 2005, pp. 9–12.

[3] R. I. C. Chiang, G. B. Rowe, and K. W. Sowerby, "A quantitative analysis of spectral occupancy measurements for cognitive radio," in *Proc. IEEE 65th VTC—Spring*, Apr. 2007, pp. 3016–3020.

[4] M. Wellens, J. Wu, and P. Mähönen, "Evaluation of spectrum occupancy in indoor and outdoor scenario in the context of cognitive radio," in *Proc. 2nd Int. Conf. CrowCom*, Aug. 2007, pp. 1–8.

[5] M. H. Islam, C. L. Koh, S. W. Oh, X. Qing, Y. Y. Lai, C. Wang, Y.-C. Liang, B. E. Toh, F. Chin, G. L. Tan, and W. Toh, "Spectrum survey in Singapore: Occupancy measurements and analyses," in *Proc. 3rd Int. Conf. CrownCom*, May 2008, pp. 1–7.

[6] R. B. Bacchus, A. J. Fertner, C. S. Hood, and D. A. Roberson, "Long-term, wide-band spectral monitoring in support of dynamic spectrum access networks at the IIT spectrum observatory," in *Proc. 3rd IEEE Int. Symp. DySPAN*, Oct. 2008, pp. 1–10.

[7] M. López-Benítez, A. Umbert, and F. Casadevall, "Evaluation of spectrum occupancy in Spain for cognitive radio applications," in *Proc. IEEE 69th VTC—Spring*, Apr. 2009, pp. 1–5.

[8] M. López-Benítez, F. Casadevall, A. Umbert, J. Pérez-Romero, J. Palicot, C. Moy, and R. Hachemani, "Spectral occupation measurements and blind standard recognition sensor for cognitive radio networks," in *Proc. 4th Int. Conf. CrownCom*, Jun. 2009, pp. 1–9.

[9] S. Pagadarai and A. M. Wyglinski, "A quantitative assessment of wireless spectrum measurements for dynamic spectrum access," in *Proc. 4th Int. Conf. CrownCom*, Jun. 2009, pp. 1–5.

[10] K. A. Qaraqe, H. Celebi, A. Gorcin, A. El-Saigh, H. Arslan, and M. S. Alouini, "Empirical results for wideband multidimensional spectrum usage," in *Proc. IEEE 20th Int. Symp. PIMRC*, Sep. 2009, pp. 1262–1266.

[11] A. Martian, I. Marcu, and I. Marghescu, "Spectrum occupancy in an urban environment: A cognitive radio approach," in *Proc. 6th AICT*, May 2010, pp. 25–29.

[12] R. Schiphorst and C. H. Slump, "Evaluation of spectrum occupancy in Amsterdam using mobile monitoring vehicles," in *Proc. IEEE 71st VTC—Spring*, May 2010, pp. 1–5.

[13] V. Valenta, R. Maršálek, G. Baudoin, M. Villegas, M. Suarez, and F. Robert, "Survey on spectrum utilization in Europe: Measurements, analyses and observations," in *Proc. 5th Int. Conf. CROWNCOM*, Jun. 2010, pp. 1–5.

[14] J. Do, D. M. Akos, and P. K. Enge, "L and S bands spectrum survey in the San Francisco bay area," in *Proc. PLANS*, Apr. 2004, pp. 566–572.

[15] P. G. Steffes and A. J. Petrin, "Study of spectrum usage and potential interference to passive remote sensing activities in the 4.5 cm and 21 cm bands," in *Proc. IEEE IGARSS*, Sep. 2004, vol. 3, pp. 1679–1682.

[16] M. Biggs, A. Henley, and T. Clarkson, "Occupancy analysis of the 2.4 GHz ISM band," *Proc. Inst. Elect. Eng.—Commun.*, vol. 151, no. 5, pp. 481–488, Oct. 2004.

[17] S. W. Ellingson, "Spectral occupancy at VHF: Implications for frequency-agile cognitive radios," in *Proc. IEEE 62nd VTC—Fall*, Sep. 2005, vol. 2, pp. 1379–1382.

[18] S. D. Jones, E. Jung, X. Liu, N. Merheb, and I.-J. Wang, "Characterization of spectrum activities in the U.S. public safety band for opportunistic spectrum access," in *Proc. 2nd IEEE Int. Symp. DySPAN*, Apr. 2007, pp. 137–146.

[19] R. de Francisco and A. Pandharipande, "Spectrum occupancy in the 2.36–2.4 GHz band: Measurements and analysis," in *Proc. 16th EW Conf.*, Jun. 2010, pp. 231–237.

[20] M. Matinmikko, M. Mustonen, M. Höyhtyä, T. Rauma, H. Sarvanko, and A. Mämmelä, "Distributed and directional spectrum occupancy measurements in the 2.4 GHz ISM band," in *Proc. 7th ISWCS*, Sep. 2010, pp. 976–980.

[21] C. Jackson, "Dynamic sharing of radio spectrum: A brief history," in *Proc. 1st IEEE Int. Symp. DySPAN*, Nov. 2005, pp. 445–466.

[22] Q. Zhao and B. M. Sadler, "A survey of dynamic spectrum access," *IEEE Signal Process. Mag.*, vol. 24, no. 3, pp. 78–89, May 2007.

[23] M. M. Buddhikot, "Understanding dynamic spectrum access: Taxonomy, models and challenges," in *Proc. 2nd IEEE Int. Symp. DySPAN*, Apr. 2007, pp. 649–663.

[24] I. F. Akyildiz, W.-Y. Lee, M. C. Vuran, and S. Mohanty, "NeXt generation/dynamic spectrum access/cognitive radio wireless networks: A survey," *Comput. Netw.*, vol. 50, no. 13, pp. 2127–2159, Sep. 2006.

[25] J. Mitola and G. Q. Maguire, "Cognitive radio: Making software radios more personal," *IEEE Pers. Commun.*, vol. 6, no. 4, pp. 13–18, Aug. 1999.

[26] S. Haykin, "Cognitive radio: Brain-empowered wireless communications," *IEEE J. Sel. Areas Commun.*, vol. 23, no. 2, pp. 201–220, Feb. 2005.

[27] R. Tandra, A. Sahai, and S. M. Mishra, "What is a spectrum hole and what does it take to recognize one?," *Proc. IEEE*, vol. 97, no. 5, pp. 824–848, May 2009.

[28] A. Attar, O. Holland, T. Farnham, M. Sooriyabandara, M. R. Nakhai, and A. H. Aghvami, "Cognitive radio techniques in heterogeneous wireless access networks," in *Heterogeneous Wireless Access Networks: Architectures and Protocols*. New York: Springer-Verlag, 2009.

[29] Z. Ahmed, H. Jamal, S. Khan, R. Mehboob, and A. Ashraf, "Cognitive communication device for vehicular networking," *IEEE Trans. Consum. Electron.*, vol. 55, no. 2, pp. 371–375, May 2009.

[30] X. Y. Wang and P.-H. Ho, "A novel sensing coordination framework for CR-VANETs," *IEEE Trans. Veh. Technol.*, vol. 59, no. 4, pp. 1936–1948, May 2010.

[31] D. Niyato, E. Hossain, and P. Wang, "Optimal channel access management with QoS support for cognitive vehicular networks," *IEEE Trans. Mobile Comput.*, vol. 10, no. 4, pp. 573–591, Apr. 2011.

[32] M. López-Benítez and F. Casadevall, "Spatial duty cycle model for cognitive radio," in *Proc. 21st Annu. IEEE Int. Symp. PIMRC*, Sep. 2010, pp. 1629–1634.

[33] M. López-Benítez and F. Casadevall, "Statistical prediction of spectrum occupancy perception in dynamic spectrum access networks," in *Proc. IEEE ICC*, Jun. 2011, pp. 1–6.

[34] M. López-Benítez and F. Casadevall, "Discrete-time spectrum occupancy model based on Markov chain and duty cycle models," in *Proc. 5th IEEE Int. Symp. DySPAN*, May 2011, pp. 90–99.

[35] H. Nan, T.-I. Hyon, and S.-J. Yoo, "Distributed coordinated spectrum sharing MAC protocol for cognitive radio," in *Proc. 2nd IEEE Int. Symp. DySPAN*, Apr. 2007, pp. 240–249.

[36] S. Huang, X. Liu, and Z. Ding, "On optimal sensing and transmission strategies for dynamic spectrum access," in *Proc. 3rd IEEE Int. Symp. DySPAN*, Oct. 2008, pp. 1–5.

[37] L. Yang, L. Cao, and H. Zheng, "Proactive channel access in dynamic spectrum networks," in *Proc. 2nd Int. Conf. CrownCom*, Aug. 2007, pp. 487–491.

[38] M. Hamid, A. Mohammed, and Z. Yang, "On spectrum sharing and dynamic spectrum allocation: MAC layer spectrum sensing in cognitive radio networks," in *Proc. 2nd Int. Conf. CMC*, Apr. 2010, pp. 183–187.

[39] C. Guo, T. Peng, Y. Qi, and W. Wang, "Adaptive channel searching scheme for cooperative spectrum sensing in cognitive radio networks," in *Proc. IEEE WCNC*, Apr. 2009, pp. 1–6.

[40] D. Datla, R. Rajbanshi, A. M. Wyglinski, and G. J. Minden, "Parametric adaptive spectrum sensing framework for dynamic spectrum access networks," in *Proc. 2nd IEEE Int. Symp. DySPAN*, Apr. 2007, pp. 482–485.

[41] Y. Pei, A. T. Hoang, and Y.-C. Liang, "Sensing-throughput tradeoff in cognitive radio networks: How frequently should spectrum sensing be carried out?" *Proc. IEEE 18th Int. Symp. PIMRC*, Sep. 2007, pp. 1–5.

[42] Y. Xu, J. Wang, and Q. Wu, "Interference-throughput tradeoff in dynamic spectrum access: Analysis based on discrete-time queuing subjected to bursty preemption," in *Proc. 4th Int. Conf. CrownCom*, Jun. 2009, pp. 1–6.

[43] Z. Liang and D. Zhao, "Quality of service performance of a cognitive radio sensor network," in *Proc. IEEE ICC*, May 2010, pp. 1–5.

[44] S. Geirhofer, L. Tong, and B. M. Sadler, "A measurement-based model for dynamic spectrum access in WLAN channels," in *Proc. IEEE MILCOM*, Oct. 2006, pp. 1–7.

[45] S. Geirhofer, L. Tong, and B. M. Sadler, "Dynamic spectrum access in WLAN channels: Empirical model and its stochastic analysis," in *Proc. 1st Int. Workshop TAPAS*, Aug. 2006, pp. 1–10.

[46] S. Geirhofer, L. Tong, and B. M. Sadler, "Dynamic spectrum access in the time domain: Modeling and exploiting white space," *IEEE Commun. Mag.*, vol. 45, no. 5, pp. 66–72, May 2007.

[47] L. Stabellini, "Quantifying and modeling spectrum opportunities in a real wireless environment," in *Proc. IEEE WCNC*, Apr. 2010, pp. 1–6.

[48] M. Wellens, J. Riihijärvi, and P. Mähönen, "Empirical time and frequency domain models of spectrum use," *Phys. Commun.*, vol. 2, no. 1/2, pp. 10–32, Mar. 2009.

[49] H. Kim and K. G. Shin, "Efficient discovery of spectrum opportunities with MAC-layer sensing in cognitive radio networks," *IEEE Trans. Mobile Comput.*, vol. 7, no. 5, pp. 533–545, May 2008.

[50] P. K. Tang and Y. H. Chew, "Modeling periodic sensing errors for opportunistic spectrum access," in *Proc. IEEE 72nd VTC—Fall*, Sep. 2010, pp. 1–5.

[51] A. Motamedi and A. Bahai, "MAC protocol design for spectrum-agile wireless networks: Stochastic control approach," in *Proc. 2nd IEEE Int. Symp. DySPAN*, Apr. 2007, pp. 448–451.

[52] Q. Zhao, L. Tong, A. Swami, and Y. Chen, "Decentralized cognitive MAC for opportunistic spectrum access in ad hoc networks: A POMDP framework," *IEEE J. Sel. Areas Commun.*, vol. 25, no. 3, pp. 589–600, Apr. 2007.

[53] P. N. Anggraeni, N. H. Mahmood, J. Berthod, N. Chaussonniere, L. My, and H. Yomo, "Dynamic channel selection for cognitive radios with heterogeneous primary bands," *Wireless Pers. Commun.*, vol. 45, no. 3, pp. 369–384, May 2008.

[54] R. Urgaonkar and M. J. Neely, "Opportunistic scheduling with reliability guarantees in cognitive radio networks," *IEEE Trans. Mobile Comput.*, vol. 8, no. 6, pp. 766–777, Jun. 2009.

[55] M. Sharma, A. Sahoo, and K. D. Nayak, "Channel selection under interference temperature model in multi-hop cognitive mesh networks," in *Proc. 2nd IEEE Int. Symp. DySPAN*, Apr. 2007, pp. 133–136.

[56] P. J. Kolodzy, "Interference temperature: A metric for dynamic spectrum utilization," *Int. J. Netw. Manage.*, vol. 16, no. 2, pp. 103–113, Mar. 2006.

[57] H. Lee and D.-H. Cho, "VoIP capacity analysis in cognitive radio system," *IEEE Commun. Lett.*, vol. 13, no. 6, pp. 393–395, Jun. 2009.

[58] H. Lee and D.-H. Cho, "Capacity improvement and analysis of VoIP service in a cognitive radio system," *IEEE Trans. Veh. Technol.*, vol. 59, no. 4, pp. 1646–1651, May 2010.

[59] P. Wang, D. Niyato, and H. Jiang, "Voice-service capacity analysis for cognitive radio networks," *IEEE Trans. Veh. Technol.*, vol. 59, no. 4, pp. 1779–1790, May 2010.

[60] T. Yücek and H. Arslan, "A survey of spectrum sensing algorithms for cognitive radio applications," *IEEE Commun. Surveys Tuts.*, vol. 11, no. 1, pp. 116–130, First Quarter, 2009.

[61] D. D. Ariananda, M. K. Lakshmanan, and H. Nikookar, "A survey on spectrum sensing techniques for cognitive radio," in *Proc. 2nd Int. Workshop CogART*, May 2009, pp. 74–79.

[62] D. Noguet, K. Haghighi, Y. Alemseged Demessie, L. Biard, A. Bouzegzi, M. Debbah, P. Jallon, M. Laugeois, P. Marques, M. Murroni, J. Palicot, C. Sun, S. Thilakawardana, and A. Yamaguchi, "Sensing techniques for cognitive radio—State of the art and trends," IEEE SCC 41 P1900.6 White paper, Oct. 2009.

[63] H. Urkowitz, "Energy detection of unknown deterministic signals," *Proc. IEEE*, vol. 55, no. 4, pp. 523–531, Apr. 1967.

[64] M. López-Benítez and F. Casadevall, "Methodological aspects of spectrum occupancy evaluation in the context of cognitive radio," *Eur. Trans. Telecommun.*, vol. 21, no. 8, pp. 680–693, Dec. 2010.

[65] M. López-Benítez and F. Casadevall, "A radio spectrum measurement platform for spectrum surveying in cognitive radio," in *Proc. 7th Int. ICST Conf. TridentCom*, Mar. 2011, pp. 1–16.

[66] O. C. Ibe, *Markov Processes for Stochastic Modeling*. New York: Academic, 2009.

[67] Z. Wang and S. Salous, "Spectrum occupancy statistics and time series models for cognitive radio," *J. Signal Process. Syst.*, vol. 62, no. 2, pp. 145–155, Feb. 2011.

[68] D. Chen, S. Yin, Q. Zhang, M. Liu, and S. Li, "Mining spectrum usage data: A large-scale spectrum measurement study," in *Proc. 15th ACM Annu. Int. Conf. MobiCom*, Sep. 2009, pp. 13–24.

[69] D. Willkomm, S. Machiraju, J. Bolot, and A. Wolisz, "Primary users in cellular networks: A large-scale measurement study," in *Proc. 3rd IEEE Int. Symp. DySPAN*, Oct. 2008, pp. 1–11.

[70] L. M. Correia, D. Zeller, O. Blume, D. Ferling, Y. Jading, I. Gódor, G. Auer, and L. van der Perre, "Challenges and enabling technologies for energy aware mobile radio networks," *IEEE Commun. Mag.*, vol. 48, no. 11, pp. 66–72, Nov. 2010.

[71] V. Blaschke, H. Jaekel, T. Renk, C. Kloeck, and F. K. Jondral, "Occupation measurements supporting dynamic spectrum allocation for cognitive radio design," in *Proc. 2nd Int. Conf. CrownCom*, Aug. 2007, pp. 50–57.

[72] A. Papoulis and S. U. Pillai, *Probability, Random Variables, and Stochastic Processes*, 4th ed. Boston, MA: McGraw-Hill, 2002.

[73] P. Kumaraswamy, "A generalized probability density function for double-bounded random processes," *J. Hydrol.*, vol. 46, no. 1/2, pp. 79–88, Mar. 1980.

[74] M. Abramowitz and I. A. Stegun, *Handbook of Mathematical Functions With Formulas, Graphs, and Mathematical Tables,* 10th ed. New York: Dover, 1972.

[75] M. C. Jones, "Kumaraswamy's distribution: A beta-type distribution with some tractability advantages," *Stat. Methodol.*, vol. 6, no. 1, pp. 70–81, Jan. 2009.

[76] W. H. Press, S. A. Teukolsky, W. T. Vetterling, and B. P. Flannery, *Numerical Recipes: The Art of Scientific Computing,* 3rd ed. Cambridge, U.K.: Cambridge Univ. Press, 2007.

Miguel López-Benítez (S'08) received the B.Sc. and M.Sc. degrees (with first-class honors) in telecommunications engineering from the Universidad Miguel Hernández (UMH), Elche, Spain, 2003 and 2006. He is currently working toward the Ph.D. degree in telecommunications engineering with the Department of Signal Theory and Communications (TSC), Universitat Politècnica de Catalunya (UPC), Barcelona, Spain.

From February 2003 to July 2006, he collaborated in several Spanish national and regional research projects in what today is the Ubiquitous Wireless Communications Research (Uwicore) Laboratory, UMH. In September 2006, he joined the Mobile Communication Research Group, TSC, UPC, where he collaborates as a Research and Teaching Assistant with the support of an FPU grant from the Spanish Ministry of Education and Science. He has been actively involved in the European-funded projects Advance Resource Management Solutions for Future All IP Heterogeneous Mobile Radio Environments (AROMA), Network of Excellence in Wireless COMmunications (NEWCOM++), and Flexible and spectrum-Aware Radio Access through Measurements and modelling In cognitive Radio systems (FARAMIR), along with Spanish projects Gestión cognitiva de recursos radio y espectro radioeléctrico en redes móviles heterogéneas con provisión de calidad de servicio extremo a extremo (COGNOS) and Acceso radio cognitivo y oportunista (ARCO). His research interests include the field of mobile radio communication systems, with special emphasis on radio resource management, heterogeneous wireless systems, quality-of-service provisioning, spectrum modeling, and opportunistic/dynamic spectrum access in cognitive radio networks. For more details, please visit http://www.lopezbenitez.es.

Mr. López-Benítez was the recipient of the 2003 and 2006 University Education National Awards, a distinction from the Spanish Ministry of Education and Science to the Best National Academic Records, as well as some other distinctions from the Spanish professional association of telecommunications engineers. His M.Sc. thesis was awarded a national research prize from the France Telecom Foundation (today Orange Foundation) in the context of the 5th Archimedes University Competition, which is the main young scientist contest in Spain organized by the Spanish Ministry of Education and Science.

Fernando Casadevall (M'87) received the Engineer and Doctor Engineer degrees in telecommunications engineering from the Universitat Politècnica de Catalunya (UPC), Barcelona, Spain, in 1977 and 1983, respectively.

In 1978, he joined UPC, where he was an Associate Professor from 1983 to 1991. He is currently a Full Professor with the Department of Signal Theory and Communications, UPC. After graduation, he was concerned with equalization techniques for digital fiber-optic systems. He has also been working in the field of digital communications, with particular emphasis on digital radio and its performance under multipath propagation conditions. Over the last 15 years, he has been mainly concerned with the performance analysis and development of digital mobile radio systems. He has published around 150 technical papers in both international conferences and magazines, most of them corresponding to IEEE publications. His particular research interests include cellular and personal communication systems, multipath transceiver design (including software radio techniques), mobility, radio resource management, and end-to-end quality-of-service issues. During the last 15 years, he has participated in more than 30 research projects founded by both public and private organizations. In particular, he has actively participated in 15 research projects founded by the European Commission, being the Project Manager for three of them, namely, Advanced Radio Resource management fOr Wireless Systems (ARROWS), Evolutionary Strategies for Radio Resource Management in Cellular Heterogeneous Networks (EVEREST), and Advanced Resource Management Solutions for Future All IP Heterogeneous Mobile Radio Environments (AROMA) (see http://www.gcr.tsc.upc.edu for details).

Prof. Casadevall has been a Technical Program Committee Member for different international IEEE supported conferences and a Reviewer for several IEEE magazines. From October 1992 to January 1996, he was in charge of the Information Technology Area, National Agency for Evaluation and Forecasting (Spanish National Research Council).